Visual Neuroscience (1994), 11, 885-897. Printed in the USA.

On the directional selectivity of cells in the visual cortex to drifting dot patterns

BERNT C. SKOTTUN, JUN ZHANG, AND DAVID H. GROSOF
Department of Psychology, University of California, Berkeley

(RECEIVED September 20, 1993; ACCEPTED March 4, 1994)

Abstract

It is well established that cortical neurons frequently show different preferred drift directions for random dots and gratings. Dot stimuli often produce two preferred directions which are arranged symmetrically on either side of the preferred directions for gratings. Based on their filter properties in three-dimensional (3-D) Fourier space and on the 3-D power spectra of drifting dot patterns, we estimated the optimal direction to drifting dots for ten neurons in the striate cortex of five adult cats. These estimates frequently gave two optimal directions, one on either side of the optimal direction to gratings. The angle between the two estimated peaks increases with drift speed. Predicted and actual angles were in reasonably good agreement. We conclude, therefore, that the directional selectivity of cortical neurons to drifting random dot patterns can be understood from linear filtering properties. For this reason, the directional tuning to drifting dot patterns seems to reflect the same mechanisms that mediate the responses to sinusoidal gratings and do not require a separate directional mechanism.

Keywords: Cortical neurons, Direction, Random dots, Linearity, Drift velocity

Introduction

Drifting single dots and patterns of random dots have been used frequently to stimulate single cells in the visual cortex of cats (Hammond & MacKay, 1975, 1977; Morrone et al., 1982; Gulyás et al., 1987; Skottun et al., 1988) and monkeys (Albright 1984; Rodman & Albright, 1989; Snowden et al., 1992). Because such stimuli contain (on average) equal Fourier power at all orientations, some believe that the directional selectivity to drifting dot patterns is uncontaminated by orientation tuning. The directional selectivity to drifting bars and gratings, on the other hand, is thought to reflect a combination of orientation and direction selectivity (Hammond & MacKay, 1977; Hammond, 1978; Albright, 1984; Rodman & Albright, 1989; Wörgötter & Eysel, 1987; Zhang, 1990). A number of investigators have observed in the cat striate cortex (Hammond & MacKay, 1977; Hammond, 1978; Hammond & Reck, 1980; Hammond, 1981; Davis & Movshon, 1980; Skottun et al., 1988; Wörgötter & Eysel, 1989, 1991; Wörgötter et al., 1991; Bauer & Jordan, 1993) as well as in area MT of the monkey (Albright, 1984; Rodman & Albright, 1989) that the directional tuning of cortical cells for random dots (texture) or single spots can be different from the directional tuning for bars or gratings. The tuning curves for the dot patterns showed two approximately symmetrical peaks on each side of the optimal direction for elongated stimuli (Hammond, 1978; Hammond & Reck, 1980; Skottun et al., 1988). This difference in tuning to dots and gratings lent credence to the notion that different mechanisms mediate the tuning to these two kinds of stimuli.

Another possibility is that the angular selectivity of the response to drifting dot patterns can be understood on the basis of linear spatial and temporal filter properties (Movshon et al., 1980; Davis & Movshon, 1980; Skottun et al., 1988; Grzywacz & Yuille, 1990, 1991). According to this view, the cells respond only when frequency components of the stimuli fall within their spatial and temporal bandpass. In the present paper, we elaborate on this model and compare its predictions with the behavior of neurons in the cat striate cortex.

Methods

The neurons included in this study represent a subset of the cells studied by Skottun et al., 1988. Selection was based on two criteria: (1) a robust response to dot patterns (since it makes little sense to study the nature of a neuron's responses to dot patterns unless the cell responds reasonably well to such stimuli), and (2) the availability of a full set of orientation, spatial frequency, and temporal frequency data as well as complete direction tuning curves for dot patterns obtained at (at least two) different drift velocities. Simple and complex cells were classi-

Reprint requests to (present address): Bernt C. Skottun, Skottun Research, 273 Mather St., Piedmont, CA 94611-5154, USA.

Present address of Jun Zhang: Department of Psychology, Cognition and Perception Program, University of Michigan, 330 Packard Rd., Ann Arbor, MI 48104-2994, USA.

Present address of David H. Grosof: Department of Ophthalmology and Visual Science, Washington University Medical School, Box 8096, 660 S. Euclid Ave., St. Louis, MO 63110, USA.

fied on the basis of the relative modulation of the response to sine gratings (Skottun et al., 1991*b*). The surgical procedures were in accordance with NIH guidelines. The reader should consult Skottun et al. (1988) for a detailed description of surgical and experimental procedures.

Unlike our previous study (Skottun et al., 1988), in which more than one dot density and dot size were used, all results in the present study were obtained with patterns of bright dots of approximately 9-min arc diameter covering about 3% of a dark background. The dots were round with slightly blurred luminance profiles. Responses to the drifting dots were obtained at 24 drift directions (sampled at 15-deg intervals) covering the full 360 deg. Drift direction was changed by rotating the display. At each direction the mean spike discharge rate was measured over a stimulus duration of 10 s. (The spontaneous activity level was measured during a 10-s blank screen presentation.) The display (Tektronix 690 SR) was masked down with a 27-deg circular aperture.

Cortical cells as spatial-temporal bandpass filters

Both simple and complex cells are known to respond to stimuli that contain energy within certain relatively narrow bands of spatial (in two dimensions) and temporal frequencies (Campbell et al., 1968,1969; Tolhurst & Movshon, 1975; Movshon et al., 1978; Tolhurst & Thompson, 1981; Skottun & Freeman, 1984). The selectivity with regard to temporal frequency is typically broader than to spatial frequency (when compared in octaves) (Holub & Morton-Gibson, 1981). Furthermore, most striate cells have approximately separable spatial- and temporal-frequency tuning curves (Tolhurst & Movshon, 1975; Ikeda & Wright, 1975; Holub & Morton-Gibson, 1981).* Therefore, the power spectrum of a cell's receptive field, or "spectral receptive field," can be represented approximately in three-dimensional (3-D) frequency space (i.e. spatial frequencies along the x and y axes plus temporal frequency along the z axis) by a vertical ellipsoid centered at the cell's optimal spatial-temporal frequencies (Fig. 1). The essence of our use of this Fourier description is that an initial linear stage of spatio-temporal filtering suffices to explain much of the directional tuning of both simple and complex cells to drifting dot patterns. In the case of simple cells, the linear stage is followed by a static nonlinearity of half-wave rectification and a power function; as a result, the average firing rate monotonically increases with the half-wave rectified response of the linear stage output. Because the static nonlinearity is not itself directionally tuned, the response to any compound visual stimulus is to a large extent predictable from the neuron's response to drifting sinusoidal gratings. Complex cells are hypothesized to sum the responses of several similarly tuned simple cells (Hubel & Wiesel, 1962; Spitzer & Hochstein, 1985) and so their responsiveness, too, is limited by simple cells' initial linear filtering stage. What we dub a "linear analysis" is simply a comparison of the spatio-temporal energy spectrum of drifting dot patterns to the cell's spectral receptive field.†

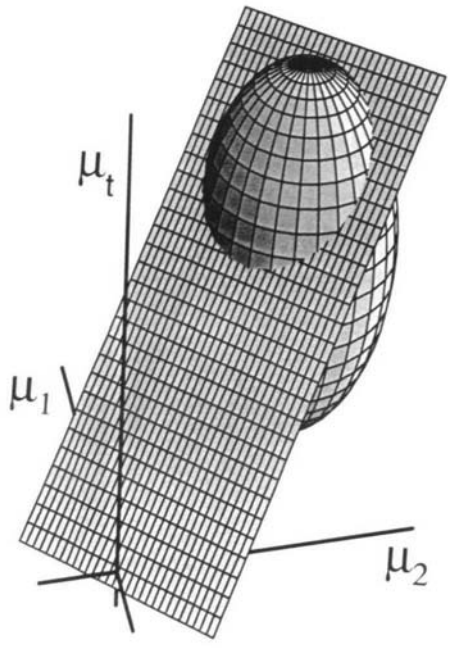

Fig. 1. The receptive field of a cortical neuron in three-dimensional frequency space. Axes μ_1 and μ_2 represent spatial frequency and the μ_t axis represents the temporal frequency. The receptive field is represented by a vertical ellipsoid (derived from the cell's responses to gratings) and the power spectrum of a moving random dot field is represented by a tilted plane (the "image plane"). The steepness or tilt of this plane is determined by the speed of the dot motion. In this figure the direction of dot drift (represented by the orientation of the plane) coincides with the optimal direction for gratings. The drift velocity was chosen so as to make the plane intersect the neuron's spectral receptive field (i.e. its receptive field in frequency space). Only the part of the plot corresponding to positive frequencies is shown.

A single dot or a pattern of random dots (or texture) has roughly equal Fourier energy at all orientations and at all spatial frequencies, subject to an upper limit set by the fineness of the pixels and a lower limit set by the overall pattern size.‡ When such a dot pattern is rigidly drifting, all of its Fourier components are moving at the same speed. Each component's temporal frequency, however, is proportional to its spatial frequency.

*Separability of the spatial and temporal FREQUENCY tuning in Fourier space does not imply spatial and temporal separability, that is, that the receptive-field sensitivity in space and time are separable functions (Emerson et al., 1987). Thus, the reader should not confuse separability of temporal- and spatial-frequency tuning curves which is well established (Tolhurst & Movshon, 1975; Ikeda & Wright, 1975; Holub & Morton-Gibson, 1981) and the spatial and temporal inseparability in the receptive field (Reid et al., 1987; Skottun, 1987; Hamilton et al., 1989) which is commonly associated with directional selectivity (Reid et al., 1987; Hamilton et al., 1989). However, spatial- and temporal-frequency separability is not critical for the present model.

†The static nonlinearity following the linear spatio-temporal filtering stage can distort the shape of the direction tuning curve, but it cannot alter the directions at which the maximum and minimum responses occur. Thus, the dot product of the stimulus and receptive-field spectra can predict the directions at which these maximum and minimum responses occur, even though the magnitude of these responses is affected by the static nonlinearity.

‡The difference between a single dot and a pattern of random dots lies in their phase spectra—in the former all Fourier components have the same relative phase while in the latter the components have random relative phases. Since phase does not affect the amplitude of a cell's response, it may be possible to adopt a single approach toward these two types of dot patterns, at least insofar as cells which are insensitive to spatial phase are concerned (i.e. Complex cells). (See also Discussion). However, the use of a single dot stimulus carries with it the serious problem of accurately mapping the receptive field so as to ensure that each passage of the single dot traverses the receptive-field center.

Consequently, lower spatial-frequency components modulate at lower temporal frequencies and higher spatial-frequency components modulate at higher temporal frequencies. The quotient of proportionality between temporal and spatial frequency expresses the velocity of the motion. (For an introduction to image motion in frequency space, see e.g. Watson & Ahumada, 1985.) The power spectrum of such drifting patterns may be geometrically represented as a plane (with evenly distributed motion energy), that is tilted away from the plane spanned by the two spatial frequency axes and toward the temporal-frequency axis (cf. Fig. 1). The intersection of this image plane with the spatial-frequency plane is a line passing through the origin perpendicular to the direction of image motion. The greater the drift speed, the steeper is the image plane. In fact, the angle of tilt depends only on image speed, regardless of direction. It follows that random dot patterns drifting at a given speed in various directions are represented by a family of planes sharing the same degree of tilt and passing through the origin. The envelope of such a family of planes is a double cone (i.e. two abutting cones) whose apex is the origin and whose axis of rotation is the temporal-frequency axis (Fig. 2). We call this the "image cone." An image cone represents what is in effect rigidly translated image motion in all directions at a given speed. Its steepness depends on the choice of drift speed—at lower speed the cone is shallower while at higher speeds it is steeper. The tangent planes of the image cone represent image motion at various directions all of the same speed. In this sense, the image cone is a compact representation of a visual stimulus drifting at all test directions.

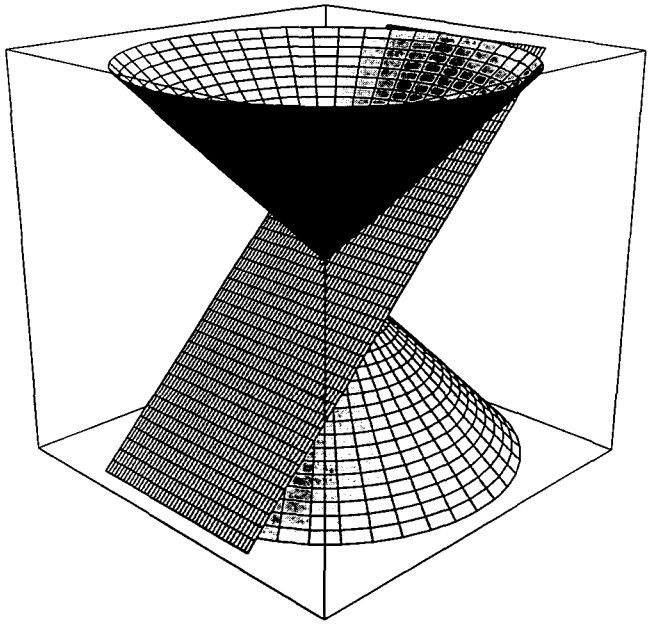

Fig. 2. The image cone of a moving dot stimulus and one of its tangent planes in spatial-temporal frequency space. Since the drifting speed determines the tilt (or steepness) of the image plane, it follows that a dot pattern moving at constant speed but at a series of different directions will yield a collection of these image planes all with identical steepness. The envelope of these planes sweeps out a double cone: the "image cone." The faster the dots drift, the tighter (that is, the more tilted toward the temporal frequency axis) is the image cone. By noting the position (in this frequency space) of a neuron's spectral receptive field relative to the image cone, one can intuitively determine whether the directional response is uni-lobed or bi-lobed.

The effect of rotating the drift direction of a rigidly drifting pattern is illustrated in Figs. 3 and 4. Fig. 3 shows two-dimensional (2-D) cross sections through Fig. 1. Panel A shows a vertical cross section while panels B and C show horizontal cross sections. Fig. 4 shows a 3-D rendition of the effect of rotating the image plane.

To highlight the essentials in the following analysis, assume for the present a cell so narrowly tuned that its ellipsoidal spectral receptive field (RF) collapses to a point in frequency space (representing the cell's preferred spatio-temporal frequency for drifting sine-wave gratings). The cell responds only if the image plane passes through this point. The essence of the present analysis is that the bifurcation in the direction tuning to dot patterns may be understood by considering the geometric location of the spectral RF point relative to the image cone representing dot patterns drifted in all directions at one speed. Slowing the dot pattern results in a shallower image cone. This may cause the RF point to lie within (i.e. above the surface of) the image cone. In this case, the cell will never be stimulated because no image plane (which is a tangential plane to the image cone) intercepts the spectral RF point, and so the cell does not respond. As drift speed is gradually increased, the cone tightens until it intercepts the spectral RF point. The speed at which this occurs is what we term the "critical speed" (see below). At this speed, there is one and only one tangent plane intercepting the spectral RF point; and the corresponding direction of dot patterns coincides with the cell's preferred direction for gratings (Fig. 5A).

When the dot speed is further increased, the image cone further tightens and the RF point now falls outside the image cone surface. In this case, there exist two tangent planes to the cone that intercept the RF point; in other words, the model cell's response peak bifurcates, producing the bi-lobed direction tuning curve (Fig. 5B) as first reported by Hammond (1978). The angular separation of these two optimal drift directions increases as the cone tightens (i.e. as the image speed increases) (Fig. 5C). A simple mathematical derivation in the Appendix shows that the angular separation δ between a dot direction peak and the preferred grating direction, which we refer to as "split angle," is given by

$$\cos\delta = v_c/v, \tag{1}$$

where v_c is the critical speed and v is the actual speed of the dot pattern. (The total angular separation between the two peaks is 2δ.) The limiting case is when the dot speed equals the critical speed, which will result in one peak only (Fig. 5A). It can be shown at the same time that the critical speed is equal to the quotient of the peak temporal frequency Ω_t over the peak spatial frequency Ω in the cell's tuning to gratings:

$$v_c = \Omega_t/\Omega. \tag{2}$$

The above formula is derived for an idealized cell with infinitely narrow tuning in the spatio-temporal frequency domain. In practice, most cortical cells are bandpass filters and have finite bandwidths of their sensitivity profiles (occupying a volume, not a point, in frequency space). Accordingly, the cells' tuning to drifting dot patterns will be somewhat different from the description given above. For instance, the two lobes of directional tuning will have some width, i.e. they will not be infinitely narrow (Fig. 6). The cells will also respond to a dot pattern drifting at a speed somewhat slower than their critical velocity,

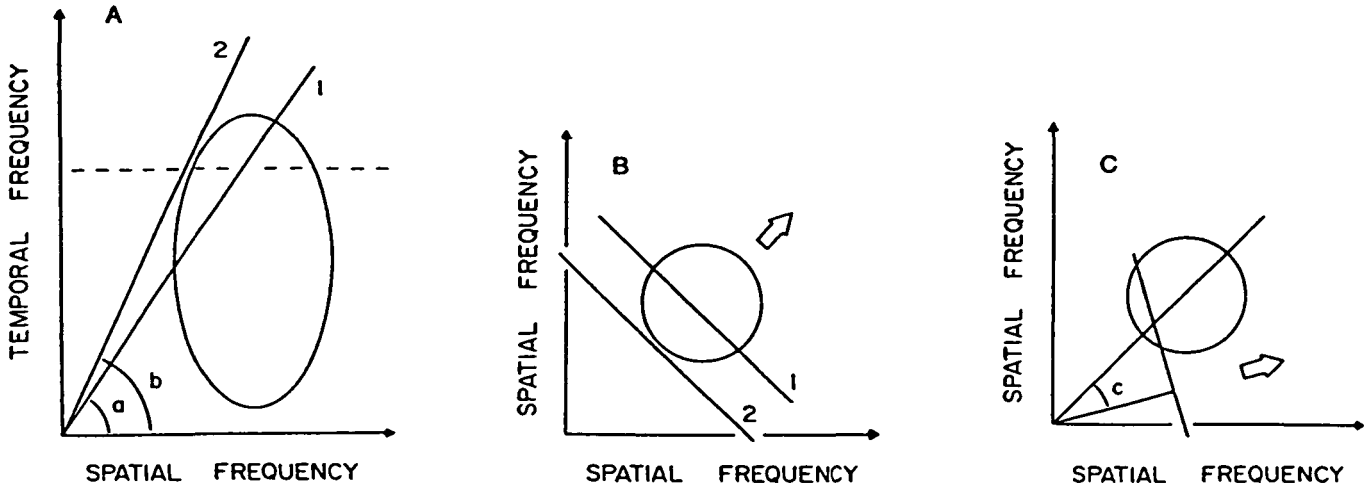

Fig. 3. Some implications of the spatio-temporal frequency model. A: A vertical cross section through the three-dimensional model (i.e. Fig. 1) perpendicular to the random dot image plane and running through the origin and the center of the spectral receptive field (represented by the ellipse). The drift velocity of the dot pattern determines the steepness of the image plane. Increasing the velocity increases the steepness of the plane. Lines 1 and 2 represent two different drift velocities. In the case of line 1, the plane intersects the spectral receptive field (as in Fig. 1). In the case of line 2, the dots are drifting too fast to activate the cell. B: A horizontal cross section through the model at the temporal frequency level indicated with a dashed line in A. The intersections between the random dot planes and the cross-section plane are indicated by two tilted solid lines marked 1 and 2. Again, we see that plane 1 does and plane 2 does not intersect the spectral receptive field (represented by the circle). (Open arrow indicates drift direction.) C: The effect of changing drift direction. In panels A and B, the dots were drifted in the optimal direction for gratings. Drifting in this direction, we saw that plane 2 did not intersect with the receptive field. However, if we were to change drift direction for this pattern 30 deg to the right (indicated by angle *c*), the same plane would run through the circle representing the cell's receptive field (in frequency space) and would thus activate the cell. (The solid line with a slope of 1 passes through the center of the spectral receptive field and indicates the optimal drift directions for gratings.) A similar case would obtain if the drift direction were to shift 30 deg to the left. Therefore, under these conditions this cell would be activated with dots drifting both to the right and left of the optimal direction for gratings, but not when the drift direction for dots is the same as the optimal direction for gratings. The result is a bi-lobed direction tuning curve.

in which case there is only one peak, of course. These observations may be accounted for when one considers the finite nature of a cell's spectral-sensitivity profile. Interestingly, Grzywacz and Yuille (1990) proved mathematically that if the spatial and temporal envelopes of the cell's receptive field follow a 3-D Gaussian function (with spatially isotropic falloff), then the two peak directions are still exactly given by eqn. (1), and critical speed given by eqn. (2). We here report our own analysis of the more general case of spatially anisotropic falloff, in which the aspect ratio is not unity. We show in the Appendix that eqns. (1) and (2) no longer hold and that when the RF is elongated (in the space domain) along the preferred orientation axis, the two peaks are actually closer than predicted by eqn. (1). Conversely, the two peaks are actually more widely separated than given by eqn. (1) when the RF elongation is perpendicular to the preferred orientation axis of the cell. Thus future attempts to quantify random dot directional tuning with linear filtering models should incorporate estimates of the aspect ratio.

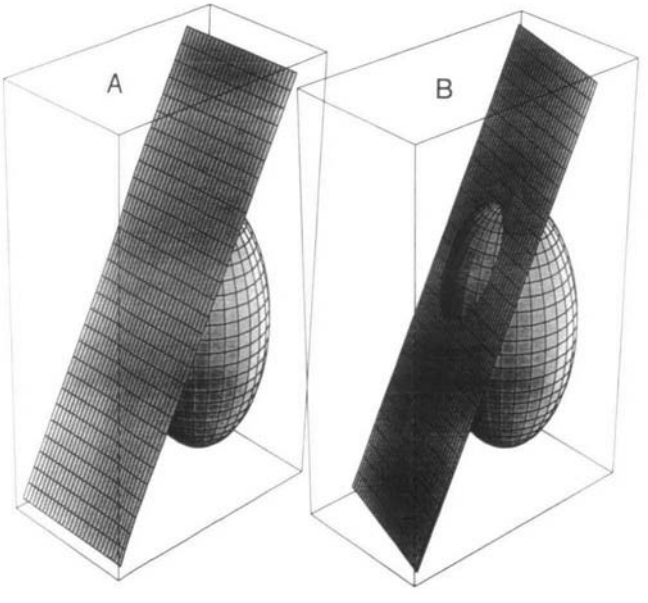

Fig. 4. The effects of changing drift direction. In panel A, the dot pattern is drifting in the direction optimal for gratings but its velocity is too high to activate the cell—the plane is too steep and does not intersect the ellipsoid. In panel B, the dots are drifting at the same velocity but their drift direction has been rotated to the right. In this case, the dots activate the cell since the image plane now intersects the ellipsoid. (This figure is essentially a 3-D rendition of the relationship described in Fig. 3.)

Results

Complete directional tuning curves for random dot patterns at two or more drift speeds were obtained for ten cells in area 17 and in the 17/18 border region of the visual cortex of five adult cats. Of the ten cells, five were simple and five complex. Directional tuning curves for one complex cell and one simple cell are shown in Figs. 7 and 8, respectively. In both figures, panel A illustrates the directional selectivity to a sinusoidal

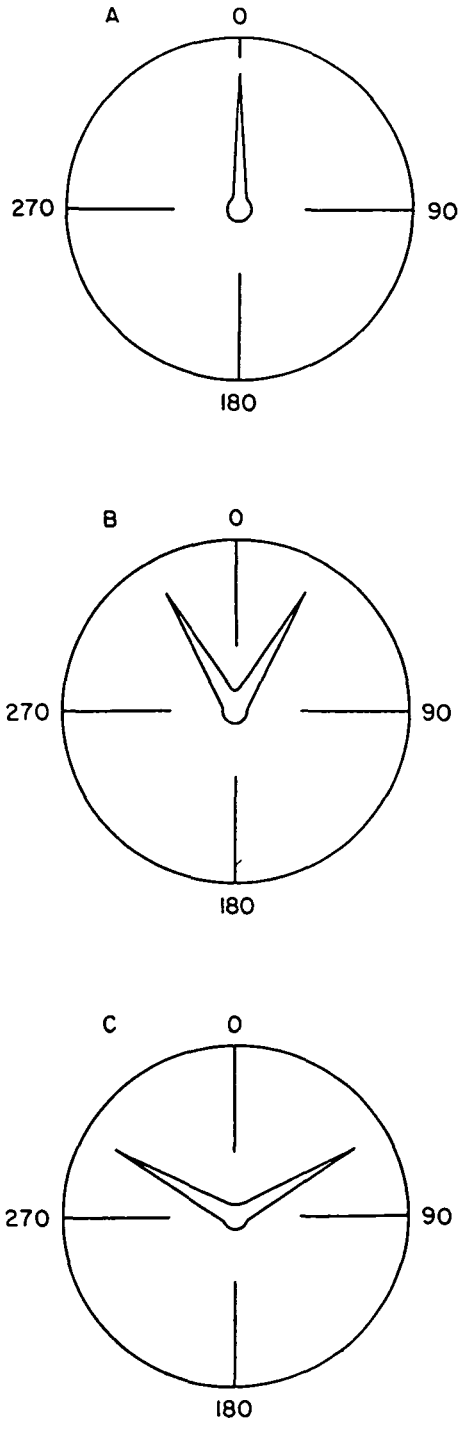

Fig. 5. Polar plots of response of an idealized cell to moving dot patterns. The cell is assumed to have very narrow tuning to spatial and temporal frequencies. Specifically, the cell will only respond to a grating of spatial frequency Ω drifting at temporal frequency $-\omega_t$. This cell will not respond to dot patterns no matter what direction the dots drift if the dot speed is less than a critical velocity. A: At the critical speed $v_c = \Omega_t/\Omega$, the cell will only respond to the dots drifting at its preferred direction for gratings. B: When dot speed increases, the cell will not respond to the dots drifting at its preferred direction for the grating. Instead, it responds to patterns drifted at two other directions (bifurcation of the peaks). The two peaks are symmetric with respect to the cell's preferred direction for gratings. Their separation is dependent on the dot speed. C: At a higher dot speed, the peaks separate further. The exact relationship between dot speed and peak separation is given in eqn. (1).

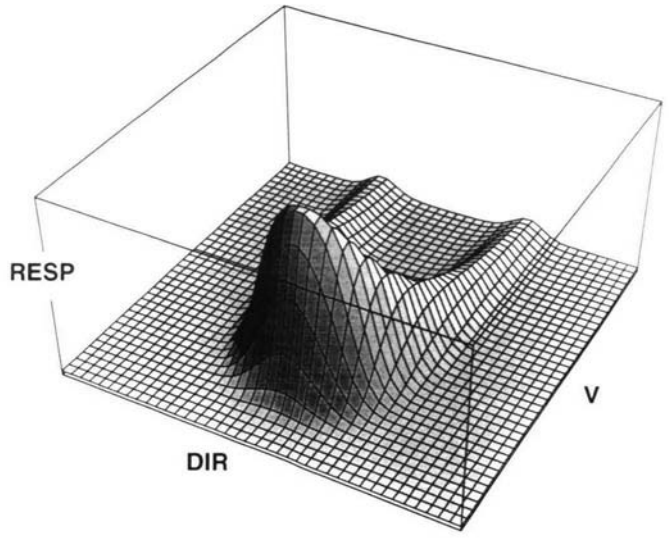

Fig. 6. Results of simulating the response (RESP) as a function of drift velocity (*V*) and drift direction (*DIR*). These simulations were carried out for a cell with finite isotropic tuning widths. Again we see that when the velocity is low the response is represented by a single peak which is located at the optimal direction for sine gratings. When the velocity is increased the cell responds at two distinct directions. The separation between these peaks increases with velocity.

grating of near-optimal spatial and temporal frequencies. Panels B, C, and D show the directional selectivity to dot patterns drifting at increasing speeds. In Fig. 7, panels B, C, and D show directional tuning curves obtained with dots drifting at 2, 4 and 16 deg/s, respectively. In Figs. 8B–8D, the cell was stimulated with dots drifting at 0.5, 2, and 16 deg/s, respectively. Both figures show a clear broadening of the tuning with increasing drift speed. Also evident (although somewhat less obvious in Fig. 7C) are bi-lobed directional tuning curves. Both of these observations are in agreement with previous reports (Hammond & Reck, 1980; Skottun et al., 1988).

In Fig. 9, we have plotted the angle between the preferred direction to gratings and the optimal direction to dot patterns, i.e. the "split angle," as a function of drift speed for all ten neurons. (Since the preferred directions to gratings in all cases were between the two optimal directions for gratings, we computed the average split angle by taking angular difference between the two peaks in the tuning curves and dividing it in two.) The two left-hand panels (i.e. A and C) show the results for simple cells. The right-hand panels (i.e. B and D) show the data for complex cells. All ten cells show a general tendency for the angle to increase with dot speed. This is in agreement with the prediction from the linear model.

As can also be seen from Fig. 9, there is no obvious difference between simple and complex cells. This is in general agreement with other studies which have found only minor differences between simple and complex cells with respect to their responses to dot patterns (Gulyás et al., 1987; Skottun et al., 1988, 1991*a*; Casanova, 1993; Bauer & Jordan, 1993). The fact that complex cell's behavior can be predicted from linear principles should not be taken to imply that these neurons are linear, but only that this aspect of their behavior can be understood from linear principles. The fact that simple and complex cells are similar in their direction selectivity to dots is consistent with a

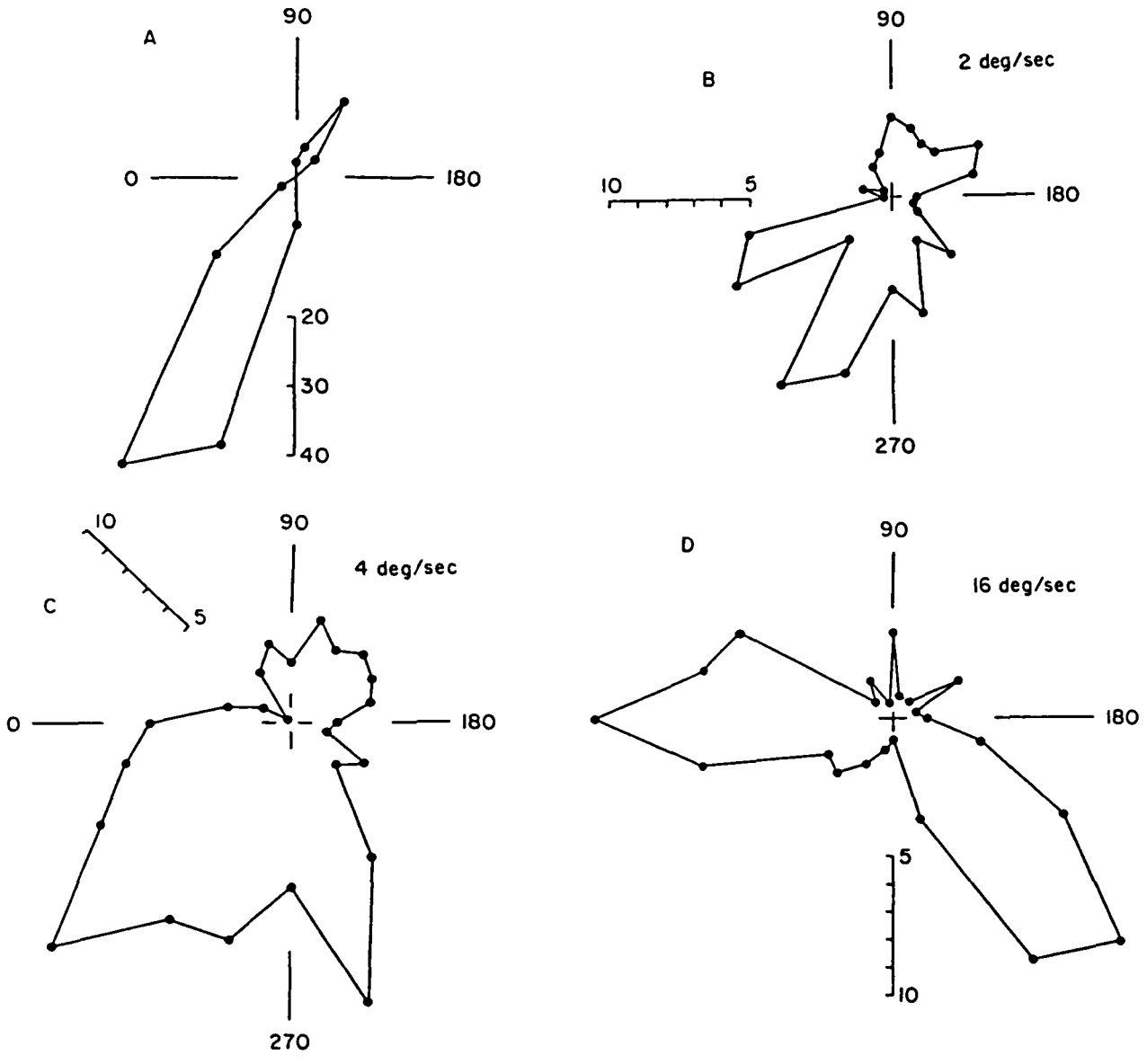

Fig. 7. Directional selectivity for one complex cell determined with sine gratings of 1.6 cycles/deg drifted at 2 Hz (A) and with random dots drifting at 2 deg/s (B), 4 deg/s (C), and 16 deg/s (D). The directional tuning to the grating is clearly monomodal, i.e. the tuning curve shows only one lobe within a 180-deg arc, while the response to the dots are bimodal. The bimodality becomes more pronounced and the angle between the peaks of the lobes increases with velocity: the angles are 30 deg, 61 deg, and 130 deg for dot velocities of 2 deg/s, 4 deg/s, and 16 deg/s, respectively. The scale bars indicate response amplitude in spikes per second. Note that the responses to gratings and random dots are scaled differently. There was no spontaneous activity either in the grating or the dots experiments with this cell.

hierarchical model (Hubel & Wiesel, 1962) in which the tuning properties of simple cells are passed on to complex cells.

To determine the applicability of the simplified linear model, we used eqn. (1) to calculate the split angle δ for each cell, at each drift velocity. In Fig. 10, we have plotted the estimated angles against actual angles. The dashed lines represent the case where predicted angles equal the actual angles. Most data points, with some exceptions, fall close to this line. As was the case in the preceding figure, left-hand and right-hand panels represent simple and complex cells, respectively.

To obtain an estimate of how well our predictions fit the actual results, we pooled all of the data in Fig. 10 into a single scatter plot. The resulting plot is shown in Fig. 11. From this plot, we found that the actual and predicted data are well correlated ($r = 0.71$, $P < 0.001$), and that the regression line (solid line) has a slope of 0.83. The 95% confidence interval for this slope is 0.33 (Student's t-test, Zar, 1984). Since a slope of 1 is well within 0.83 ± 0.33, we conclude that our predictions and our data are in relatively good agreement.

Responses of cortical neurons undergo random fluctuations (Dean, 1981; Tolhurst et al., 1983; Bradley et al., 1987). The reader may at this point ask to what extent stimulus variation—the differences among our statistically identical random dot stimuli—affects the foregoing conclusion. Our model predicts simply the average response to the statistical property of isotropy and flatness in the random dot pattern spectra. Random

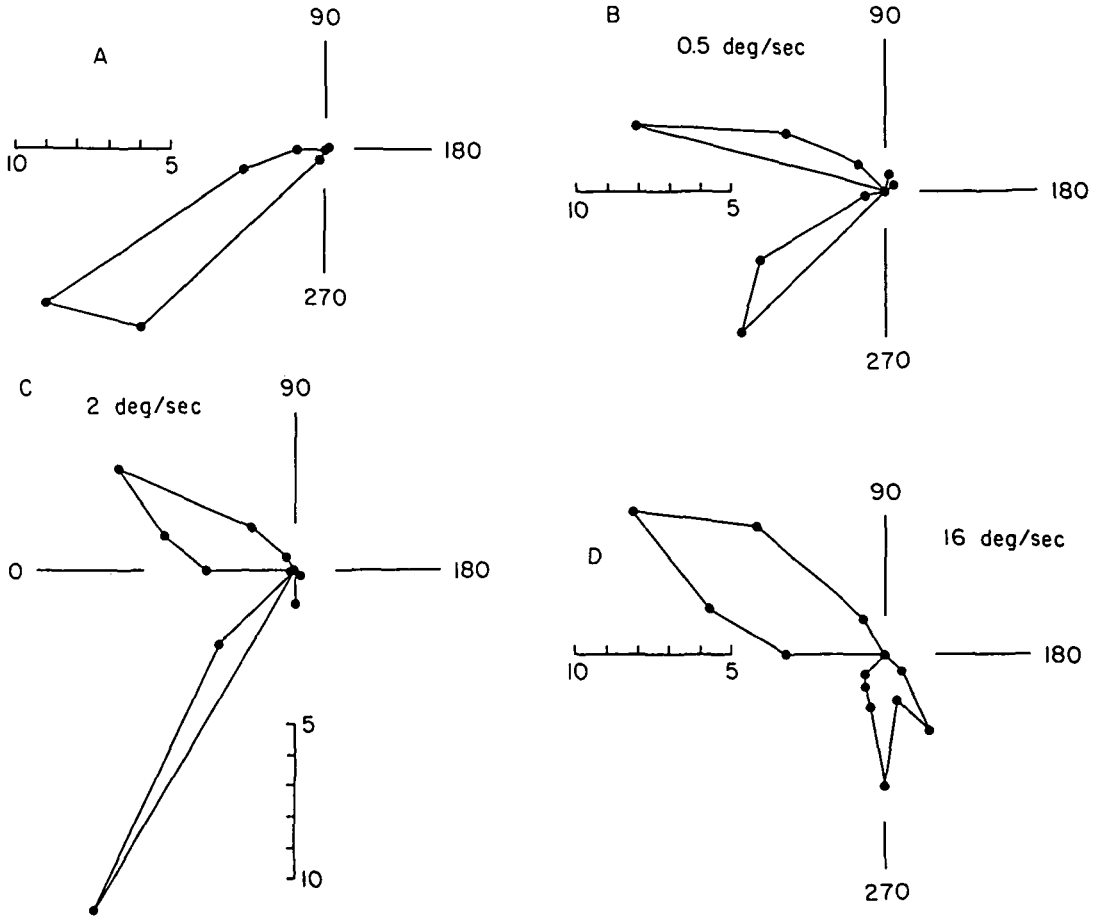

Fig. 8. Directional selectivity for one simple cell determined with sine grating of 0.7 cycle/deg drifted at 2 Hz (A) and with random dots drifted at 0.5 deg/s (B), 2 deg/s (C), and 16 deg/s (D). The angles between the lobes in panels B, C, and D were 60 deg, 90 deg, and 120 deg, respectively. There was no spontaneous activity.

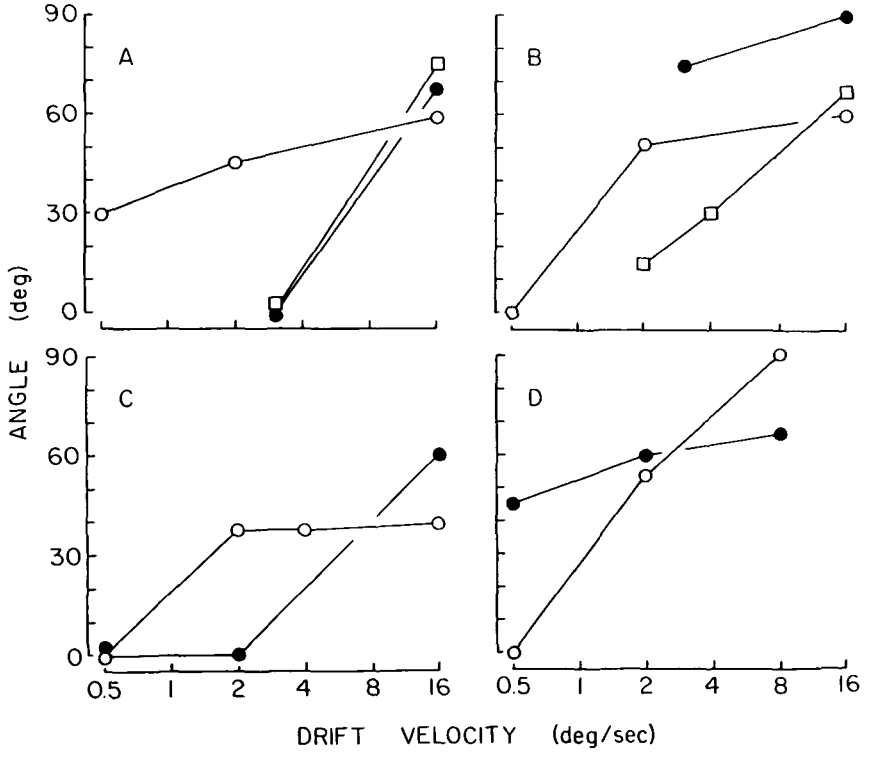

Fig. 9. Angular difference between optimal drift direction for gratings and random dot fields as a function of the dot patterns' drift velocity. Panels A and C show results for five simple cells, and B and D shows results for five complex cells. (The data for each cell class have been plotted in two panels for the sake of clarity.) The angular difference between the peak of the dot response and the peak of grating response was taken as the difference between the two lobes in the dot response tuning curves divided by two (see text). As can be seen the angular difference between preferred direction for gratings and for dots increased with velocity in all cells. (The cell shown in Fig. 8 is represented with open circles in panel A. The data for the cell in Fig. 7 are represented with open squares in B.)

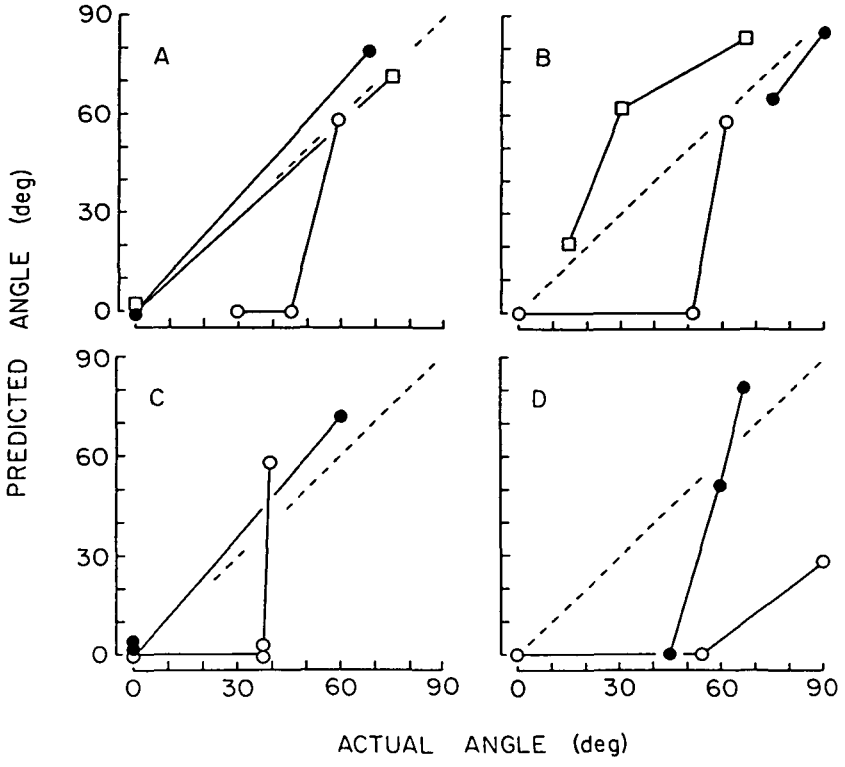

Fig. 10. Predicted split angle plotted against actual angle. Panels A and C give results for five simple cells and panels B and D represent five complex cells. The data for each cell (obtained at various velocities) are joined by straight lines and are depicted with the same symbols. The symbols in the various panels correspond to those of Fig. 9 (e.g. the cell depicted in A by filled symbols is the same as the one depicted in panel A of Fig. 9 with filled symbols, etc.). Dashed lines indicate perfect correspondence between predicted and actual angles.

deviations from that average in any one stimulus can confound the analysis; we have previously addressed the question of repeatability of directional tuning curves to different random dot stimuli. We found that the tuning curves are generally similar, but that the details of the curves often differ. (See Skottun et al., 1988, Figs. 5 and 6.) Therefore a perfect agreement between the actual and predicted data would not always be expected. This is not a problem specific to our experiment but a limitation inherent in all use of random stimuli.

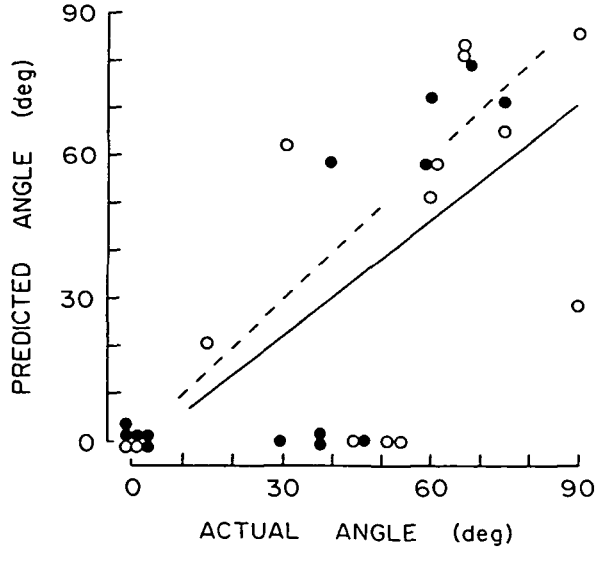

Fig. 11. Scatter plot of predicted angle against actual angle for all cells and velocities. Correlation coefficient is 0.71. The dashed line represents a slope of 1.0, i.e. perfect correspondence between predicted and actual angles. Solid line is a regression line of slope 0.83 fitted to the data. Filled and open symbols represent simple and complex cells, respectively.

An interesting feature of the data in Fig. 11 that our model does not predict is a cluster of points near the the horizontal axis. This cluster represent instances for which no peak splitting was predicted but some did occur. This could have resulted from our overestimating the critical velocity which is calculated from the temporal high frequency cutoff of the cells. This highlights the importance of accurately estimating critical velocity. We estimated this value on the basis of the spatial- and temporal-frequency tuning curves. While the optimal spatial frequency is well defined for most cells, the optimal temporal frequency and the "highest temporal frequency which gives a robust response" are often not. For this reason, we have been able to test our hypotheses in a way that does not depend on the accuracy of the estimate of "critical velocity." From eqns. (1) and (2),

$$v \cos \delta = \Omega_t / \Omega. \tag{3}$$

The left-hand side of eqn. (3), or the product of the speed of the dot pattern and the cosine of the split angle, is computable from direction tuning measurements for various dot speeds. In Fig. 12, we have plotted this product (normalized to Ω_t/Ω) as a function of the angle. According to our simplified model, this ratio should be a constant value, independent of dot speed, because the right-hand side of eqn. (3) is only determined by parameters of the cell's tuning to gratings. If the critical speed is incorrectly estimated due to experimental uncertainties, then the bias ought to be a constant, independent of dot speed. In Fig. 12, we have plotted the ratios for all ten cells. (The data are dispersed over three panels for the sake of clarity, and simple and complex cells are represented by filled and open symbols, respectively.)

Fig. 12 shows that, with only two exceptions (one of which shows no effect of angle), for each cell the ratio increases as a function of the split angle. This pattern of data cannot be explained in terms of eqn. (1) and inaccurate estimation of the

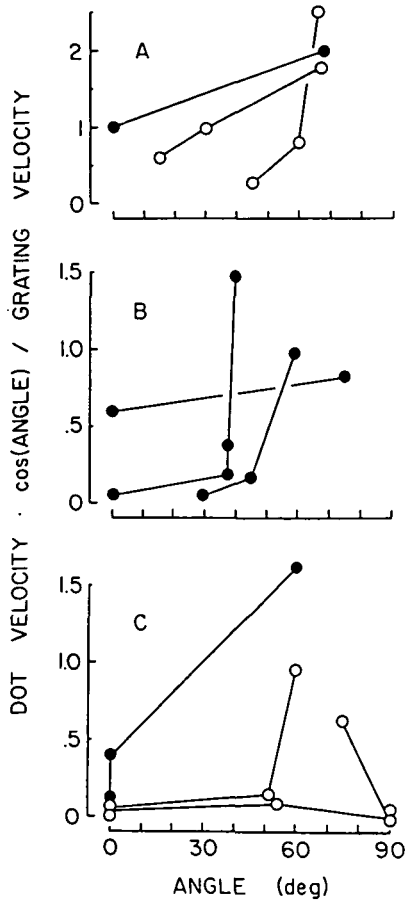

Fig. 12. The product of drift velocity for dots and cosine of the angle divided by grating velocity plotted as a function of angle. (The division serves simply to scale the results.) Again, the angle here refers to the angle between the optimal direction of drift for dots and for gratings. Filled and open symbols represent simple and complex cells, respectively.

critical speed from the grating data. Note that eqn. (1) is based on the assumption that the cell's spectral receptive field is infinitesimally narrow, or, as extended by Grzywacz and Yuille (1990), that the receptive field's falloff is a spatially isotropic Gaussian. A real cortical neuron may not follow either of these idealistic descriptions. Indeed, investigators (Webster & De Valois, 1985) have found that the aspect ratio of cat striate cell spectral RFs average 1.45, elongated along the axis of preferred orientation. We therefore investigated the effect of spectral RF anisotropy on the amount of peak split. As is shown in the Appendix, the two directional peaks can get closer or further apart depending on the way the anisotropy goes. However, it is also shown that when the anisotropy is relatively minor, the product of the dot speed and the cosine of the split angle remains a constant for individual cells. Summarizing the above arguments, it appears that the pattern of data in Fig. 12 could be due to large anisotropy in the cells' RF (i.e. aspect ratio significantly different from unity) or a nonlinear interaction between the cells' tuning to various Fourier components.

Discussion

The peak-splitting data presented in this article agree with numerous previous reports from both the cat (Hammond & MacKay, 1977; Hammond, 1978; Hammond & Reck, 1980; Hammond, 1981; Davis & Movshon, 1980; Skottun et al., 1988; Wörgötter & Eysel, 1989, 1991; Wörgötter et al., 1991; Bauer & Jordan, 1993) and the monkey (Albright 1984; Rodman & Albright, 1989; Snowden et al., 1992). We have achieved some success in explaining this phenomenon as the consequence of linear spatio-temporal filtering. In addition, the counter intuitive result of our analysis of aspect ratio detailed in the Appendix points the way to a more refined experimental study. Extending the earlier work of Grzywacz and Yuille (1990, 1991) to consider the variable of the aspect ratio, we conclude that future efforts to quantify dot direction tuning in terms of linear filtering properties should include measurement of aspect ratio. Notwithstanding the present study's lack of that measure, we find some success in explaining the basic observation of previous reports in cat striate cortex (Hammond, 1978; Davis & Movshon, 1980; Hammond & Reck, 1980; Movshon et al., 1980; Skottun et al., 1988): the optimal drift directions for dots often differ from the optimal drift directions for gratings, and this difference becomes larger with increasing drift speed. The shifts in preferred direction are in agreement with predictions based on linear properties (Davis & Movshon, 1980; Movshon et al., 1980; Grzywacz & Yuille, 1990, 1991) and with the notion of "component direction selectivity" (Movshon et al., 1980, 1985). In essence, the seemingly different response to dots and to gratings can be accounted for by linear decomposition of the dot patterns into a sum of gratings of all spatial frequencies and orientations.

Because our stimuli had a low dot density—only 3% of the surface was covered with dots—it might seem possible that some of our data were the result of unusual artifactual configurations of dots in the receptive fields, rather than reflecting the average pattern. Two reasons argue against this possibility: (1) In some cases, we repeated the experiments with stimuli of identical statistics but different dot configurations. Directional tuning curves obtained with such regenerated stimuli were generally similar, although, as one would expect, small differences in the peaks of the tuning curves were sometimes present (see Skottun et al., 1988, Figs. 5 and 6). (2) In some cells, we repeated the experiment with stimuli of 50% dot density. Although changing the density of the dots sometimes caused a substantial change in response amplitude, the directional tuning curves obtained with these stimuli were in general agreement with those obtained with 3% density (see Skottun et al., 1988, Fig. 10).

Though from a small sample of cells, the present results are in general agreement with previous findings that the quasilinear filtering properties of neurons in the cat's striate cortex and monkey's V1 allow prediction of responses to a variety of complex stimuli in terms of their sensitivity to the Fourier components of the stimuli (De Valois et al., 1979; Davis & Movshon, 1980; Movshon et al., 1980; Grosof et al., 1985; Movshon et al., 1985). A number of interesting conclusions can be drawn from these results. However, a caveat is that the present results were obtained with cells in cat area 17 and the 17/18 border area, and cells in other visual areas and in other species may respond differently.

Traditionally, the use of random dots in motion experiments was inspired by the desire to isolate pure "direction" selectivity and to avoid the influence of orientation tuning. This seemed plausible because a pattern of random dots lacks elongated form cues and contains equal energy at all orientations. It was thought, therefore, that any selectivity as to drift direction in the responses to dot patterns reflects directional mechanisms,

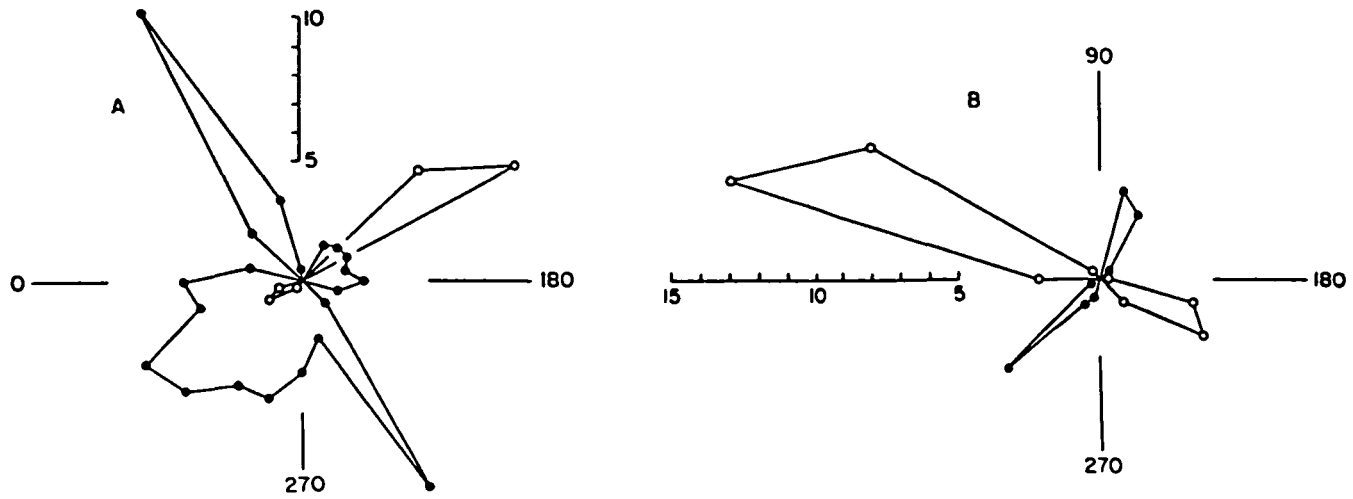

Fig. 13. Response as a function of direction for gratings (open symbols) and random dots (filled symbols) for one complex cell (A) and one simple cell (B). The complex and the simple cell were tested with random dots drifting at 8 and 16 deg/s, respectively. In both instances the peaks of the tuning curves for random dots were shifted about 90 deg away from the peaks of the tuning curves for gratings. Also, in both cases the two peaks of the random dot curves were of approximately equal amplitude. On the other hand, the amplitudes of the peaks in the grating response were highly unequal. Determined with random dots these cells would be classified as bidirectional. Determined with gratings these cells show pronounced directional bias. This illustrates that when using random dots it is possible to misclassify directionally biased neurons as bidirectional. (The scales give the response amplitudes in spikes per second.)

uncontaminated by orientation selectivity. In the present study, we were able to predict, at least to a first approximation, the directional selectivity to drifting dot patterns from the 2-D spatial-frequency tuning (which includes orientation) and the temporal tuning. Thus, to the extent that a neuronal response is dominated by oriented linear filtering, it is incorrect to regard direction selectivity to dots as separate from direction selectivity to gratings. In applying a filtering analysis to predict the dot tuning from grating tuning, it is essential to take account of both spatial and temporal filtering. The present results present a unified explanation of responses to dot patterns and so dispense with the notion that responses to spots and bars are necessarily "independent" (Wörgötter & Eysel, 1991). For the same reason, there is no need to postulate that "the depressed sensitivity" in the direction tuning curve for dot patterns at the preferred direction for bars and gratings represents inhibition from orientational mechanisms (Hammond, 1978). Our results also imply that it is unnecessary to construe the changes in preferred direction with drift speed as an indication that *directional selectivity* changes with speed (Hammond & Reck, 1980). Our analysis is consistent with directional selectivity being a fixed *property* of the cell, as opposed to being merely a description of specific results obtained under specific circumstances.§

An interesting implication of our filtering hypothesis is that a neuron which is directionally selective to gratings of optimal temporal and spatial frequency may, when tested with sufficiently fast moving random dot patterns (fast relative to the cell's critical speed), show two near-equal lobes that are about 180 deg apart (see Fig. 13). Some might be inclined to treat such a response as reason to classify the cell as directionally selective for gratings but not for dots. This approach would also cause the preferred drift direction to be misjudged by (about) 90 deg. This phenomenon illustrates the point that, rather than being particularly well-suited to probe directional tuning, random dots may be particularly difficult to use in understanding motion processing properties of visual neurons.**

Earlier studies which have related sine grating responses to

§One possible way to disentangle direction selectivity from orientation selectivity may be to follow a Fourier transform of the direction tuning curve described by Wörgötter and Eysel (1987) and Zhang (1990). This analysis, however, is suited for data obtained with oriented stimuli and should not be applied to data obtained with dots.

**Some studies of monkey MT (Albright 1984; Rodman & Albright, 1989) and cat striate cortex (Wörgötter & Eysel, 1989) have found cells that respond optimally to single dots or patterns of dots drifted in a direction orthogonal to the preferred direction for gratings. Our analysis suggests this is the expected result from spatio-temporal filtering considerations when dot speed greatly exceeds the cell's critical speed [c.f. eqn. (2)]. In this regard, it is worth noting that the speeds used in these studies were quite high: Rodman and Albright (1989) used single dots drifting at 4–32 deg/s, and Wörgötter and Eysel (1989) used drift velocities between 4 and 10 deg/s. Some of these velocities are well above the highest velocities we used (i.e. 16 deg/s), and even the lowest velocity in these studies (4 deg/s) has in our study resulted in clearly bi-lobed tuning functions for dots and in some cases close to 90-deg peak shifts. Our analysis and data are based on neurons in the cat's striate cortex. Two of the above cited studies involved area MT of the monkey (Albright 1984; Rodman & Albright, 1989). It is therefore interesting to speculate that similar mechanisms may contribute to directional tuning in monkey area MT. Since neurons in monkey visual cortex typically prefer much higher spatial frequencies and roughly similar temporal frequencies than do cat neurons, the critical speed may have been quite low for many of these neurons [see eqn. (1)]. Thus, many of the velocities used in these studies may have exceeded the critical speed of (putatively quasilinear) intrinsic MT or afferent (e.g. V1) directional neurons, thus eliciting large differences in optimal drift directions for gratings and dots. There are few quantitative experiments on the mechanisms of directional selectivity in macaque monkey as compared to the cat. A recent report (Shadlen et al., 1993) suggests that directional cells in MT simply pool local signals, making more plausible the notion that MT neurons are strongly influenced by striate-like directional mechanisms operating over relatively small subregions of the MT cells' receptive fields. If so, then it is important for investigators to examine the effect of drift speed when a difference in dot and grating direction tuning is encountered in MT as well as in V1.

responses to 2-D stimuli have typically employed simplified 2-D stimuli such as plaids or checkerboards (De Valois et al., 1979; Movshon et al., 1985). Both plaids and checkerboards have punctate spatial-frequency spectra and investigators have taken care to ensure that the temporal frequency of components inside the spatial-frequency tuning curve at all times are within the temporal bandpass (the frequency of components outside the spatial bandpass are irrelevant to a linear analysis, of course). Temporal factors have therefore not played a role in these experiments. In this respect plaid and checkerboard stimuli are highly unnatural. The dots patterns we used represent a marked step toward more naturalistic stimuli.

Random dot patterns are perhaps more naturalistic and certainly more complex than plaids and checkerboards, but they may be too complex to be the stimulus of choice to determine direction selectivity in visual mechanisms with a linear "front-end." However, these stimuli provide us with a clear demonstration of the importance of temporal factors in neuronal image motion processing.

Acknowledgments

This work was supported by grants from the National Eye Institute (EY-00014) and from the National Science Foundation (85-19613) to Professor R.L. De Valois. D.H. Grosof was supported by the National Eye Institute NRSA EY-06158.

References

ALBRIGHT, T.D. (1984). Direction and orientation selectivity of neurons in visual area MT of the macaque. *Journal of Neurophysiology* **52**, 1106-1130.

BAUER, R. & JORDAN, W. (1993). Different anisotropies for texture and grating stimuli in the visual map of cat striate cortex. *Vision Research* **33**, 1447-1450.

BRADLEY, A., SKOTTUN, B.C., OHZAWA, I., SCLAR, G. & FREEMAN, R.D. (1987). Visual orientation and spatial frequency discrimination: A comparison of single neurons and behavior. *Journal of Neurophysiology* **57**, 755-772.

CAMPBELL, F.W., CLELAND, B.G., COOPER, C.F. & ENROTH-CUGELL, C. (1968). The angular selectivity of visual cortical cells to moving gratings. *Journal of Physiology* **198**, 237-250.

CAMPBELL, F.W., COOPER, C.F. & ENROTH-CUGELL, C. (1969). The spatial selectivity of the visual cells of the cat. *Journal of Physiology* **203**, 223-235.

CASANOVA, C. (1993). Responses of cells in cat's area 17 to random dot patterns: Influence of stimulus size. *NeuroReport* **4**, 1011-1014.

DAVIS, E.T. & MOVSHON, J.A. (1980). Direction selectivity in cortical complex cells. *Investigative Ophthalmology and Visual Science* (Suppl.) **19**, 223-224.

DEAN, A.F. (1981). The variability of discharge of simple cells in the cat striate cortex. *Experimental Brain Research* **44**, 437-440.

DE VALOIS, K.K., DE VALOIS, R.L. & YUND, E.W. (1979). Responses of striate cortex cells to grating and checkerboard patterns. *Journal of Physiology* **291**, 483-505.

EMERSON, R.C., CITRON, M.C., VAUGH, W.J. & KLEIN, S.A. (1987). Nonlinear directionally selective subunits in complex cells of cat striate cortex. *Journal of Neurophysiology* **58**, 33-65.

FAHLE, M. & POGGIO, T. (1981). Visual hyperacuity: Spatiotemporal interpolation in human vision. *Procedings of the Royal Society B* (London) **213**, 451-477.

GROSOF, D.H., SKOTTUN, B.C. & DE VALOIS, R.L. (1985). Linearity of cat cortical cells: Responses to 2-D stimuli. *Investigative Ophthalmology and Visual Science* (Suppl.) **26**, 265.

GRZYWACZ, N.M. & YUILLE, A.L. (1990). A model for the estimate of local image velocity by cells in the visual cortex. *Procedings of the Royal Society B* (London) **239**, 129-161.

GRZYWACZ, N.M. & YUILLE, A.L. (1991). Theories for the visual perception of local velocity and coherent motion. In *Computational Models of Visual Processing*, ed. LANDY, M.S. & MOVSHON, J.A., pp. 231-252. Cambridge, Massachusetts: MIT Press.

GULYÁS, B., ORBAN, G.A., DUYSENS, J. & MAES, H. (1987). The suppressive influence of moving textured backgrounds on responses of cat striate neurons to moving bars. *Journal of Neurophysiology* **57**, 1767-1791.

HAMILTON, D.B., ALBRECHT, D.G. & GEISLER, W.S. (1989). Visual cortical receptive fields in monkey and cat: Spatial and temporal phase transfer function. *Vision Research* **29**, 1285-1308.

HAMMOND, P. (1978). Directional tuning of complex cells in area 17 of the feline visual cortex. *Journal of Physiology* **285**, 479-491.

HAMMOND, P. (1981). Simultaneous determination of directional tuning of complex cells in cat striate cortex for bar and texture motion. *Experimental Brain Research* **41**, 364-369.

HAMMOND, P. & MACKAY, D.M. (1975). Differential responses of cat visual cortical cells to textured stimuli. *Experimental Brain Research* **22**, 427-430.

HAMMOND, P. & MACKAY D.M. (1977). Differential responsiveness of simple and complex cells in cat striate cortex to visual texture. *Experimental Brain Research* **30**, 275-296.

HAMMOND, P. & RECK, J. (1980). Influence of velocity on directional tuning of complex cells in cat striate cortex for texture motion. *Neuroscience Letters* **19**, 309-314.

HOLUB, R.A. & MORTON-GIBSON, M. (1981). Response of visual cortical neurons of the cat to moving sinusoidal gratings: Response-contrast functions and spatio-temporal interactions. *Journal of Neurophysiology* **46**, 1244-1259.

HUBEL, D.H. & WIESEL, T.N. (1962). Receptive fields, binocular interaction and functional architecture in the cat's visual cortex. *Journal of Physiology* (London) **160**, 106-154.

IKEDA, H. & WRIGHT, M.J. (1975). Spatial and temporal properties of 'sustained' and 'transient' neurones in area 17 of the cat's visual cortex. *Experimental Brain Research* **22**, 363-383.

MORRONE, M.C., BURR, D.C. & MAFFEI, L. (1982). Functional implications of cross-orientation inhibition of cortical visual cells. I. Neurophysiological evidence. *Proceedings of the Royal Society B* (London) **216**, 335-354.

MOVSHON, J.A., DAVIS, E.T. & ADELSON, E.H. (1980). Directional movement selectivity in cortical complex cells. *Society for Neuroscience Abstracts* **6**, 670.

MOVSHON, J.A., THOMPSON, I.D. & TOLHURST, D.J. (1978). Spatial and temporal contrast sensitivity of neurones in areas 17 and 18 of the cat's visual cortex. *Journal of Physiology* **283**, 101-120.

MOVSHON, J.A., ADELSON, E.H., GIZZI, M.S. & NEWSOME, W.T. (1985). The analysis of moving visual patterns. In *Pattern Recognition Mechanisms* ed. CHAGAS, C., GATTASS, R. & GROSS, C., pp. 117-151. The Vatican: Pontificia Academia Scientiarium.

REID, R.C., SOODAK, R.E., & SHAPLEY, R.M. (1987). Linear mechanisms of direction selectivity in simple cells of cat striate cortex. *Proceedings of the National Academy of Science*, **84**, 8740-8744.

RODMAN, H.R. & ALBRIGHT, T.D. (1989). Single-unit analysis of pattern-motion selective properties in the middle temporal visual area (MT). *Experimental Brain Research* **75**, 53-64.

SHADLEN, M.N., NEWSOME, W.T. & ZOHARY, E. (1993). Integration of local motion signals in area MT. *Society of Neuroscience Abstracts* **19**, 1282.

SKOTTUN, B.C. (1987). *Neurophysiology and perception: Studies of the visual system*. Ph.D. Dissertation, University of California, Berkeley.

SKOTTUN, B.C. & FREEMAN, R.D. (1984). Stimulus specificity of binocular cells in the cat's visual cortex: Ocular dominance and the matching of left and right eyes. *Experimental Brain Research* **56**, 206-216.

SKOTTUN, B.C., GROSOF, D.H. & DE VALOIS, R.L. (1988). Responses of simple and complex cells to random dot patterns: A quantitative comparison. *Journal of Neurophysiology* **59**, 1719-1735.

SKOTTUN, B.C., GROSOF, D.H. & DE VALOIS, R.L. (1991*a*). Letter to the editors—On the responses of simple and complex cells to random dot patterns. *Vision Research* **31**, 43-46.

SKOTTUN, B.C., DE VALOIS, R.L., GROSOF, D.H., MOVSHON, J.A., ALBRECHT, D.G. & BONDS, A.B. (1991*b*). Minireview—Classifying simple and complex cells on the basis of response modulation. *Vision Research* **31**, 1079-1086.

SNOWDEN, R.J., TREUE, S. & ANDERSEN, R.A. (1992). The response of neurons in areas V1 and MT of the alert rhesus monkey to moving random dot patterns. *Experimental Brain Research* **88**, 389-400.

SPITZER, H. & HOCHSTEIN, S. (1985). A complex-cell receptive field model. *Journal of Neurophysiology* **53**, 1266-1286.

TOLHURST, D.J. & MOVSHON, J.A. (1975). Spatial and temporal contrast sensitivity of striate cortical neurones. *Nature* **257**, 674-675.

TOLHURST, D.J. & THOMPSON, I.D. (1981). On the variety of spatial frequency selectivities shown by neurons in the area 17 of the cat. *Proceedings of the Royal Society B* (London) **213**, 183–199.
TOLHURST, D.J., MOVSHON, J.A. & DEAN, A.F. (1983). The statistical reliability of signals in single neurons in cat and monkey visual cortex. *Vision Research* **23**, 775–785.
WATSON, A.B. & AHUMADA, A.J. (1985). Model of human visual-motion sensing. *Journal of the Optical Society of America A* **2**, 322–341.
WEBSTER, M.A. & DE VALOIS, R.L. (1985). Relationship between spatial-frequency and orientation tuning of striate-cortex cells. *Journal of the Optical Society of America A* **2**, 1124–1132.
WÖRGÖTTER, F. & EYSEL, U.T. (1987). Quantitative determination of orientational and directional components in the response of visual cortical cells to moving stimuli. *Biological Cybernetics* **57**, 349–355.
WÖRGÖTTER, F. & EYSEL, U.T. (1989). Axis of preferred motion is a function of bar length in visual cortical receptive fields. *Experimental Brain Research* **76**, 307–314.
WÖRGÖTTER, F. & EYSEL, U.T. (1991). Axial responses in visual cortical cells: Spatio-temporal mechanisms quantified by Fourier components of cortical tuning curves. *Experimental Brain Research* **83**, 656–664.
WÖRGÖTTER, F., MUCHE, T. & EYSEL, U.T. (1991). Correlations between directional and orientational tuning of cells in cat striate cortex. *Experimental Brain Research* **83**, 665–669.
ZAR, J.H. (1984). *Biostatistical Analysis*. 2nd edition, Englewood Cliffs, New Jersey: Prentice-Hall, Inc.
ZHANG, J. (1990). How to unconfound directional and orientational information in visual neuron's response. *Biological Cybernetics* **63**, 135–142.

Appendix

We follow Watson and Ahumada (1985) to derive eqns. (1) and (2) (see *Cortical Cells as Spatial Temporal Filters*) from the basic notions of Fourier analysis of image and image motion. It has been pointed out (e.g. by Fahle & Poggio, 1981; Watson & Ahumada, 1985) that image velocity (v_1, v_2) is related to the individual Fourier component with spatial frequency (μ_1, μ_2) and temporal frequency μ_t through the following equation:††

$$\mu_t = (v_1\mu_1 + v_2\mu_2) \tag{A1}$$

This defines an image plane in the frequency domain. The ideal cell with infinitely narrow (delta-function) tuning is represented as a single point in frequency space $(\Omega_1, \Omega_2, \Omega_t) = (\Omega\cos\theta, \Omega\sin\theta, \Omega_t)$, with θ and Ω being the cell's preferred orientation and preferred spatial frequency, respectively. For the cell to respond, the image plane must pass through this point:

$$\Omega_t = (\Omega_1 v_1 + \Omega_2 v_2) \tag{A2}$$

A dot pattern drifting with speed v and direction α has velocity vector $(v_1, v_2) = (v\cos\alpha, v\sin\alpha)$. For the dot stimulus to activate the cell,

$$\Omega_t = \Omega v\cos(\alpha - \theta) \tag{A3}$$

Defining the split angle $\delta = \alpha - \theta$ and critical speed $v_c = \Omega_t/\Omega$, we have

$$\cos\delta = v_c/v \tag{A4}$$

††There is actually a negative sign on the left-hand side in this equation, indicating the fact that a rightward drifting image has negative temporal frequencies for its positive spatial frequencies. Here we use the unsigned value of temporal frequency and thereby omit this apparently awkward negative sign.

If the dot speed v is smaller than v_c, the right-hand side of eqn. (A4) is greater than one, and there will never be a solution for δ. In this case, the ideal cell will give no response no matter which direction the dot pattern drifts. When v is greater than v_c, eqn. (A4) will have two possible solutions of δ, a positive and a negative one. This is to say, there will be two drift directions (or two values of α) that elicit a response from the cell. Furthermore, these two directions are symmetric with respect to θ, the optimal drift direction for gratings. The greater the v, the smaller the right-hand side of eqn. (A4), and the further away α is from θ (or the further apart the two peaks). This explains the empirically observed "peak splitting" in the cell's tuning to drifting dot patterns (Figs. 5, 7, and 8).

The above conclusion is for an ideal cell with infinitely narrow spatio-temporal tuning. Grzywacz and Yuille (1991) considered a model where the receptive fields of cortical cells have Gaussian falloffs in both spatial and temporal frequencies (i.e. Gabor tuning functions). These authors derived the cell's response to a dot pattern assuming that the spatial Gaussian tapering is isotropic. Interestingly, it was shown that the amount of peak-split was exactly the same as for the ideal cell with infinitely narrow tuning, as given by eqn. (A4). However, if the Gaussian falloff is anisotropic, the peak splitting is different.

In the following, we discuss the effect of receptive-field anisotropy on the peak separation associated with a cell's response to drifting dot patterns. We follow Grzywacz and Yuille's derivation and show that for a cell with anisotropic receptive-field falloff the average response N to a dot pattern drifting in direction α is

$$N(\alpha) = \frac{1}{\sigma_1^2\sigma_2^2 + (\sigma_1^2 v_2^2 + \sigma_2^2 v_1^2)\sigma_t^2} \times \exp\left(-\frac{\sigma_1^2\sigma_2^2\sigma_t^2(\Omega_1 v_1 + \Omega_2 v_2 - \Omega_t)^2}{\sigma_1^2\sigma_2^2 + (\sigma_1^2 v_2^2 + \sigma_2^2 v_1^2)\sigma_t^2}\right) \tag{A5}$$

For simplicity (and biological plausibility), we assume that either the major or minor axis of the anisotropic Gaussian coincides with the preferred orientation of the cell. We denote the two widths of Gaussian falloff as σ_1, σ_2, representing spatial frequency and orientation bandwidths, respectively. Substituting in Ω, the cell's preferred spatial frequency, we can derive the cell's response as

$$N(\alpha) = \frac{1}{D(\alpha)}\exp(-\sigma_1^2\sigma_2^2\sigma_t^2(\Omega v\cos\alpha - \Omega_t)^2/D(\alpha)) \tag{A6}$$

where

$$D(\alpha) = \sigma_1^2\sigma_2^2 + v^2\sigma_t^2(\sigma_1^2\sin^2\alpha + \sigma_2^2\cos^2\alpha) \tag{A7}$$

To obtain the directional peak, we calculate the derivative of $N(\alpha)$, or more conveniently, of $\log N(\alpha)$ with respect to drift angle α:

$$\frac{d\log N}{d\alpha} = \frac{\sigma_1^2\sigma_2^2\sigma_t^2}{D} 2\Omega v(\Omega v\cos\alpha - \Omega_t)\sin\alpha + \frac{\sigma_1^2\sigma_2^2\sigma_t^2(\Omega v\cos\alpha - \Omega_t)^2}{D^2}\frac{dD}{d\alpha} - \frac{1}{D}\frac{dD}{d\alpha} \tag{A8}$$

with

$$\frac{dD}{d\alpha} = v^2\sigma_t^2(\sigma_1^2 - \sigma_2^2)\sin 2\alpha \tag{A9}$$

In the case of an isotropic Gaussian, $\sigma_1 = \sigma_2$ so that $dD/d\alpha = 0$ always, and the last two terms of eqn. (A8) drop out. Thus, the directional peaks occur when $\cos\alpha = \Omega_t/\Omega v$. This result was first derived in this context by Grzywacz and Yuille (1990) as discussed earlier. When the Gaussian falloff is anisotropic, i.e. when $\sigma_1 \neq \sigma_2$, all three terms remain, and so the response $N(\alpha)$ does not peak at $\pm\alpha_0 = \pm\cos^{-1}(\Omega_t/\Omega v)$. Instead, if $\sigma_1 > \sigma_2$, we have

$$\begin{aligned}\left.\frac{d\log N}{d\alpha}\right|_{\alpha=\pm\alpha_0} &= -\frac{1}{D}\left.\frac{dD}{d\alpha}\right|_{\alpha=\pm\alpha_0} \\ &= -\left.\frac{v^2\sigma_t^2(\sigma_1^2 - \sigma_2^2)\sin(2\alpha)}{D(\alpha)}\right|_{\alpha=\pm\alpha_0} \\ &\sim \begin{cases} -\sin 2\alpha_0 < 0, & \text{for } \alpha = \alpha_0 \\ \sin 2\alpha_0 > 0, & \text{for } \alpha = -\alpha_0 \end{cases}\end{aligned} \tag{A10}$$

This implies that the peaks have been pushed toward each other. In other words, the separation of the two peaks has decreased. Of course, the converse is true when $\sigma_1 < \sigma_2$. Therefore, receptive-field anisotropy will affect the amount of peak split.

The amount of deviation of the split angle $\Delta\alpha$ can be estimated analytically if the receptive-field anisotropy is small. The Taylor expansion of $\log N(\alpha)$ at the new peak angle $\alpha_0 + \Delta\alpha$ gives

$$0 = \frac{d\log N(\alpha_0 + \Delta\alpha)}{d\alpha} = \left.\frac{d\log N}{d\alpha}\right|_{\alpha=\alpha_0} + \left.\frac{d^2\log N}{d\alpha^2}\right|_{\alpha=\alpha_0}\Delta\alpha \tag{A11}$$

Therefore,

$$\Delta\alpha = -\frac{d\log N(\alpha_0)}{d\alpha}\Big/\frac{d^2\log N(\alpha_0)}{d\alpha^2} \tag{A12}$$

Explicitly calculated,

$$\Delta\alpha = -\frac{(\sigma_1^2 - \sigma_2^2)}{\sigma_1^2\sigma_2^2\Omega^2}\left(\frac{\cos\alpha_0}{\sin\alpha_0}\right) + \mathcal{O}(\sigma_1^2 - \sigma_2^2) \tag{A13}$$

where $\mathcal{O}(\sigma_1^2 - \sigma_2^2)$ represents higher orders in $\sigma_1^2 - \sigma_2^2$, and can be omitted for minor anisotropies. We can then calculate the product of the dot speed and the cosine of the split angle

$$\begin{aligned} v\cos(\alpha_0 + \Delta\alpha) &\simeq v\cos\alpha_0 - v\sin\alpha_0\Delta\alpha \\ &= v\cos\alpha_0\left(1 + \frac{(\sigma_1^2 - \sigma_2^2)}{\sigma_1^2\sigma_2^2\Omega^2}\right) \\ &= \frac{\Omega_t}{\Omega}\left(1 + \frac{(\sigma_1^2 - \sigma_2^2)}{\sigma_1^2\sigma_2^2\Omega^2}\right) \\ &= \text{constant} \end{aligned} \tag{A14}$$

That is to say, the left-hand side remains constant at various dot speeds for any cell with minor anisotropies. Of course, if $\sigma_1 = \sigma_2$, then eqn. (A14) reduces to eqn. (3) in the Results section.